Desalination and Water Treatment
www.deswater.com
doi: 10.5004/dwt.2020.25773

194 (2020) 133–142
August

Simple iron-based sludge processing for low-cost, efficient heavy metal adsorbent (the case study)

Michal Hegedüs[a], Alexandra Bekényiová[b,*], Katarína Harčárová[a], Petr Lacina[a], Zuzana Danková[b,c], Simona Matejová[d], Anton Zubrik[b], Erika Tóthová[b]

[a]*GEOtest, a.s., Šmahova 1244/112, 627 00 Brno, Czech Republic, emails: hegedus@geotest.cz (M. Hegedüs), harcarova.katka@gmail.com (K. Harčárová), lacina@geotest.cz (P. Lacina)*
[b]*Institute of Geotechnics, Slovak Academy of Sciences, Watsonova 45, 040 01 Košice, Slovak Republic, Tel. +421 55 792 26 24; Fax: +421 55 792 26 01; emails: avaskova@saske.sk (A. Bekényiová), zuzana.dankova@geology.sk (Z. Danková), zubant@saske.sk (A. Zubrik), etothova@saske.sk (E. Tóthová)*
[c]*Department of Applied Technology of Raw Materials, State Geological Institute of Dionýz Štúr, Regional Centre Košice, Jesenského 8, 040 01 Slovak Republic*
[d]*Institute of Inorganic Chemistry, Technology and Materials, Faculty of Chemical and Food Technology, Slovak University of Technology, Radlinského 9, 812 37 Bratislava, Slovak Republic, email: matejovasimona@gmail.com (S. Matejová)*

Received 27 September 2019; Accepted 28 February 2020

ABSTRACT

This paper presents a scalable method for the conversion of iron-based sludge obtained as a side-product of wastewater treatment technology into a readily applicable adsorbent for toxic ions removal from aqueous environments. In the first step, iron-based sludge was prepared with a neutralized acidic iron(III) sulfate solution which was added into industrial wastewater. After dehydration, a sample was calcinated at 500°C. The prepared magnetic material contained approximately 50% iron in a form of nanocrystalline maghemite/magnetite composite mixture. scanning electron microscopy and Brunauer–Emmett–Teller measurements showed that the material was composed of micrometric agglomerates of non-porous nanocrystallites with a specific surface area of 66 m^2/g. This iron-based sludge adsorbent was used for real wastewater treatment. Despite the quantity of competitive toxic ions present, approximately 50% of the present arsenate oxyanion could be removed without previous wastewater pre-treatment. Compared to the real water sample, maximum uptake of As(V) from the model solution was ca 23% higher. The rate of adsorption was also comparably higher for the model solution with k = 0.273 g/mg/min.

Keywords: Wastewater treatment; Sludge processing; Iron-based adsorbent; Maghemite/magnetite composite; Toxic ions removal

1. Introduction

Iron-based materials, particularly in the form of nanoparticles, have been studied for years due to their excellent sorption properties. For example, naturally occurring iron oxides, for example, hematite (α-Fe_2O_3), maghemite (γ-Fe_2O_3), and magnetite (Fe_3O_4) have recently been gaining attention [1]. Not only do their nanoparticles possess a high surface area, but they also represent a low-cost alternative to many other available sorbents on the market. In addition, they can easily be separated from the water after the sorption process using magnets. Until now, many synthetic methods have successfully been used to synthesize nanoparticles of iron oxides for water treatment.

For example, Hu et al. [2] synthesized γ-Fe_2O_3 nanoparticles with a specific surface area of 198 m^2/g and an average particle size of 10 nm via hydrothermal route. They demonstrated fast kinetics of Pb(II), Ni(II) ions removal

* Corresponding author.

with high sorption capacity. A similar study was carried out by Cheng et al. [3] with maghemite nanoparticles prepared by co-precipitation and calcination at 650°C with a slightly larger diameter of approximately 60 nm. Biochar/γ-Fe_2O_3 composite prepared by pyrolysis was reported by Zhang et al. [4] with the arsenic sorption capacity of 4.2 mg/g. In comparison to the study of Wu et al. [5] where nanocrystalline γ-Fe_2O_3 has been encapsulated in a mesoporous carbon matrix also by pyrolysis, a much lower sorption capacity was achieved. Surprisingly, even higher arsenic sorption capacity was found for solvothermally prepared flower-like α-Fe_2O_3 nanoparticles with a specific surface of 130 m^2/g (up to 51 mg/g for As(V)) [6]. Thus, it can be concluded that in addition to the specific surface area, the morphology of the prepared sorbent particles plays a key role as well. Several attempts have also been made on the utilization of ferrites $M^{II}Fe_2O_4$ (M^{II} = Fe, Mn, Cu, Co, Ni, and Zn) as heavy metal removers [7]. Mixed-valence oxides were prepared by co-precipitation of corresponding metal salts with subsequent calcination at 400°C. Overall, high sorption capacity mainly for Cr(VI) species was observed through the whole series. Whereas the commercially available $Fe^{II}Fe^{III}{}_2O_4$ (magnetite) nanoparticles do not exhibit any extraordinary sorption properties [8,9], magnetite nanoparticles coated with humic acid, which were prepared by co-precipitation method, showed sorption capacities up to 100 mg/g for selected metals [10]. Even higher arsenic (248 mg/g) uptake was achieved using starch-bridged magnetite nanoparticles prepared in the same way [11]. Unfortunately, in many cases an in-depth analysis of the materials not reported and the economic aspect of the syntheses is not considered. Additionally, several problems connected with nanoparticles utilization must be addressed in respect to their large-scale deployment:

- impact of the nanoparticles on human health has not been investigated in detail yet [12],
- nanoparticles stabilization is required in order to maintain a high surface area (additional reactants or synthesis steps needed),
- up-scaling of multi-step nanoparticles synthesis may be technologically challenging [13].

In spite of this, and the current global trend to establish a regenerative system, also known as a circular economy, we have proposed a simple and technologically achievable process of iron-based sludge recycling from wastewater treatment technology. The resulting nanocrystalline composite material was tested for its adsorption properties of As(V) from aqueous environments and the results are outlined below.

2. Experimental

2.1. Material

The iron-based sludge was formed as a by-product of industrial wastewater treatment technology for adsorbable organic halides (AOX) removal applied in a textile factory located in the Czech Republic. The process of water treatment is schematically depicted in Fig. 1 and can be described as follows:

- In the first step, anionic surfactants SYNTEFIX TE along with iron(III) sulfate reagents (PREFLOC) were pumped into the tanks containing industrial wastewater.
- The pH value was then adjusted up to 6–7 by the addition of $Ca(OH)_2$ water suspension by constant stirring.
- The mixture containing precipitated sludge was transferred to a sedimentation tank. For the better settlement of the precipitate, a flocculant (SOKOFLOK brand) was added as a 0.1% solution.
- The sludge was then filter pressed to obtain a solid product in the form of dark brown pellets.

The pellets were crushed with a mortar, and a sieved fraction of particles (<1 mm) was annealed for a different time and temperature in corundum crucibles. After annealing, the material was further milled for 10 min using a vibratory ball mill (Janetzki-KM1, Poland), equipped with an agate mortar

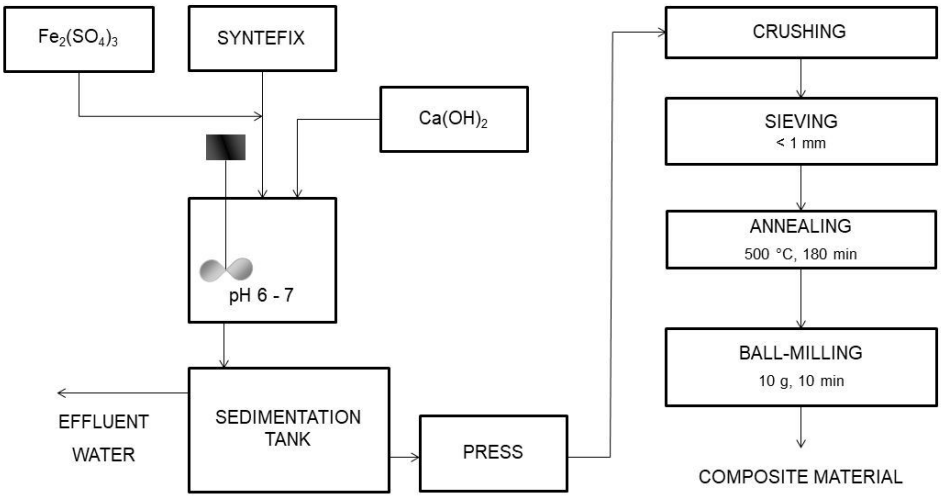

Fig. 1. Schematic representation of water treatment technology and processing of the iron-based sludge.

and one milling ball to increase its homogeneity. The selected sample, annealed at 500°C for 180 min (denoted as IBA500), was characterized in detail and used for adsorption tests.

2.2. Characterization

2.2.1. X-ray diffractometry

The X-ray powder diffraction patterns were collected by a Philips PW1820 automated powder diffractometer with Bragg–Brentano parafocusing geometry using CoKα radiation (40 kV, 35 mA) equipped with automatic divergent slit and curved graphite monochromator placed in the diffracted beam. Each pattern was measured over the 2θ range of 15°–80° with a step size of 0.03° and a counting time 2 s per step at room temperature. Samples of iron-based sludge were first ground using an agate mortar and pestle and were then added to a Si zero-background sample holder. Phase identification was performed using Match! software, with a complete COD reference database package.

2.2.2. X-ray fluorescence spectrophotometry

Portable X-ray fluorescence (XRF) spectrometer DELTA PROFESSIONAL (Innov-X, Canada) was used for on-site analysis and sludge classification. Two energetically different exciting beams (40 eV for 60 s, 15 eV for 30 s) were used for analysis, primarily for determination of the following elements: P, S, Cl, K, Ca, Ti, Mn, Fe, and Sb. The results were used for the evaluation of elemental composition, focusing on the iron content in pressed sludge.

2.2.3. Scanning electron microscopy

The morphology of the surface was observed by a field-emission scanning electron microscopy (FE-SEM) of type TESCAN MIRA 3 (Tescan, Czech Republic) equipped with the energy dispersive X-ray (EDX) detector (Oxford Instruments).

2.2.4. Specific surface area measurements

An additional method for the particle size determination, the surface and porous properties of the IBA500 sample, were studied by physical adsorption of nitrogen performed by the NOVA 1200 apparatus (Quantachrome, USA) at 77 K. Before the measurement, the sample was activated in vacuum at 200°C over 18 h. The experimental data were processed by the BET (Brunauer–Emmett–Teller) isotherm in the range of relative pressure 0.05–0.2 p/p_0 to obtain the value of the specific surface area. The value of total pore volume V_a was estimated from the maximum adsorption at relative pressure close to the saturation pressure. The pore size distribution was calculated using the BJH (Barret–Joyner–Hallenda) method from the desorption isotherm.

2.2.5. Thermal analysis

Thermal stability of the pellets dried at 70°C for 24 h was carried out using an STA 449 Jupiter thermal analyzer (Netzsch, Germany). Approximately 85 mg of the sample was placed into an Al_2O_3 crucible and heated from 70°C to 900°C with a rate of 30°C/min in air atmosphere.

2.2.6. Zeta potential analyses

Zeta Potential (ZP) was measured using a Zetasizer Nano ZS (Malvern Panalytical Ltd., United Kingdom). The Zetasizer Nano measures the electrophoretic mobility of particles. Malvern Zetasizer software was used for evaluation. The data for electrophoretic mobility were converted into the zeta potential using Henry's equation and Smoluchowski approximation. Smoluchovski approximation is valid for polar media and particles >200 nm. Sample ZP (concentration of 2 g/L) was measured in deionized water within various pH ranges, adjusted by the addition of 1 M NaOH or HNO_3. The measurements were repeated three times.

2.2.7. ICP-AES measurements

The levels of selected metals in the real water sample were determined to utilize ICP-OES spectrometer iCAP 7400 D (Thermo Scientific, Germany) equipped with a CID86 detector. The instrument was calibrated on the certified reference material AN 9090(MN), representing a mixture of metal ions stabilized in 5% HNO_3 (v/v). For experiments performed with model solutions, the levels of toxic elements before and after the adsorption were determined by atomic absorption spectroscopy (AAS) using spectrometer 240 RS/2400 (Varian, Australia).

2.3. Adsorption tests

The adsorption tests were performed with real wastewater (pH = 7.50, conductivity = 1,205 μS/cm) obtained from an abandoned mining site near the city Pezinok in Slovakia. It is well-known that the input concentration of As(V) in real wastewater may be dependent on the time of the sampling, therefore fresh wastewater was used for each experiment. The concentration ranged from approximately 800 up to 1,100 μg/L. The amounts of other detected metals by ICP-AES analysis are listed in Table 1.

Table 1
Composition of the real wastewater obtained from the abandoned mining site near the city Pezinok in Slovakia

Element	Concentration (μg/L)	Parameter	Value
As	880	pH	7.50
Ca	186,000	Conductivity	1,205 μS/cm
Cd	7.21	Cl^-	22 mg/L
Cu	4.34	F^-	0.2 mg/L
K	5,170	HCO_3^-	226 mg/L
Mg	74,200	NH_4^+	0.48 mg/L
Mn	302	NO_2^-	0.12 mg/L
Na	19,300	NO_3^-	<3 mg/L
Ni	26	PO_4^{3-}	0.23 mg/L
Sb	455	SO_4^{2-}	584 mg/L
Zn	8.50	COD-Mn	1.27 mg/L

Table 2
Amounts of selected elements determined by on-site XRF measurement

Sample	Element – ppm (ug/g)									
	P	S	Cl	K	Ca	Ti	Mn	Fe	Sb	∑C, H, N, O
No. 1	2,549	6,025	2,365	1,445	454	1,601	318	219,196	379	xxx
No. 2	2,345	5,925	1,970	1,357	<LOD	1,590	299	208,222	334	xxx
No. 3	2,646	6,484	1,703	1,240	831	1,598	318	225,290	352	xxx
No. 4	2,797	7,248	1,731	1,258	489	1,726	310	218,626	456	xxx
Average	2,584	6,421	1,942	1,325	366	1,629	311	217,834	380	xxx
Percentage	0.26%	0.64%	0.19%	0.13%	0.03%	0.16%	0.03%	21.70%	0.04%	76.82%

To compare the adsorption effect of the IBA500 sample towards the As(V) without other influences (ionic strength, competitive ions, selectivity toward other elements, which are present in the real wastewater), the model solution was also studied. A model solution of As(V) was prepared from Na_2HAsO_4 (per analysis quality) and deionized water, in the concentration of 1 mg As(V)/L.

The influence of pH, adsorbent dose, and contact time on the adsorption properties was studied. The pH of the solution was treated by diluted HNO_3 and NaOH to be 5 and 7. The adsorption experiments were performed as batch tests. Suspensions of the real wastewater/model solution and the dosed adsorbent were shaken in a rotary shaker in glass bottles at laboratory temperature (20°C).

All adsorption experiments were duplicated. The products were separated by filtration and the filtrates were analyzed for residual As(V) content by AAS.

3. Results and discussion

3.1. Material characterization and processing

In order to evaluate the elemental composition of a fresh, pressed sludge, on-site XRF measurements were carried out and the results for selected elements are shown in Table 2.

The amount of iron for each sample varied approximately 20%–22% and its value was only affected by the addition of a $Ca(OH)_2$ suspension, necessary for pH value adjustment during the operation. Among other *d*-metal elements, significant amounts of titanium were found. That is attributed as an impurity originating from the industrial production of iron(III) sulfate reagent. Antimony, as the only toxic element, was also detected in treated wastewater and may represent a potential drawback of material implementation under highly acidic/basic conditions, where soluble antimony species exist. Relatively high content of some non-metallic elements (P, S, and Cl) may have been caused by the following:

- sulfate ions from $Fe_2(SO_4)_3$ which are precipitated upon neutralization in the form of gypsum,
- adsorbed organic compounds from treated wastewater (chlorine atoms possibly from AOX),
- impurity salts found in an industrial iron(III) sulfate reagent.

Thermal behavior of dried sludge pellets illustrates Fig. 2a. Due to the complexity of the studied system and high heating rate, not all processes can be clearly resolved from the provided TG/DTG curves. In lower temperatures range (25°C–500°C), removal of adsorbed moisture and chemically bonded water molecules might be observed. These are found mostly in polyhydroxo complexes of iron and calcium sulfate dihydrate, formed upon neutralization of acidic sulfate solution. In this temperature range, significant mass loss (ca 45%) is observed. Such a reduction in total mass

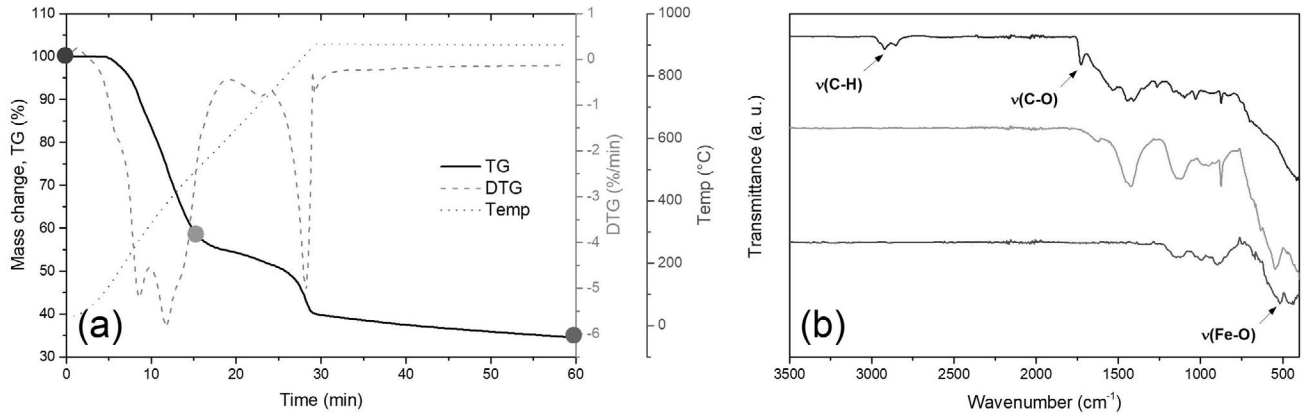

Fig. 2. TA/DTG curves of iron sludge (a) and IR spectra corresponding to marked points on TG curve (b).

must be unambiguously connected with the decomposition of organic compounds present in all samples (please refer to infrared spectra).

High temperatures (above 500°C) show only one significant mass loss at approximately 860°C which is assumed to be connected with the decomposition of calcium carbonate possibly present in industrial $Ca(OH)_2$. The presence of CO_3^{2-} anion can be detected by infrared spectroscopy, Fig. 2b. The sharp absorption peak at ca 875 1/cm should correspond to one of the vibration modes of this anion and it is not present in the sample annealed at 900°C. From the given data, it can be concluded that temperatures above 400°C–500°C are sufficient for the processing of the studied sludge.

According to the findings from the thermal analysis, the sludge was annealed at different temperatures for various times. Qualitative phase analyses of these samples were performed. The patterns were mostly dominated by anhydrous iron oxides (maghemite γ-Fe_2O_3, magnetite Fe_3O_4, and hematite α-Fe_2O_3). All samples contained approximately the same amount of anhydrite $CaSO_4$ (ca. 13%). Several weak reflections in these patterns remained unidentified. In addition, a semiquantitative phase analysis was accomplished to evaluate the influence of various temperatures on different iron oxide phases and their crystallinity. The sample annealed for 180 min at 500°C contained over half the amount of maghemite and the remainder was magnetite, anhydrite, and a minor amount of hematite (<3 wt.%). After 90 min annealing at 700°C, the sample contained about the same amount of maghemite and hematite (each ca. 30%) and the rest contained magnetite with anhydrite. Finally, the last sample annealed for 60 min at 900°C contained about 75 wt.% of hematite and the remainder was anhydrite with a minor amount of magnetite. This evolution is in accordance with the stability of iron oxides in the air. Increasing the temperature led to a continuous transformation of maghemite to the hematite phase. Higher crystallinity is achieved at high temperatures which, however negatively affects the adsorption properties. Thus, the nanocrystalline sample containing the highest amount of maghemite phase (annealed for 180 min at 500°C, further denoted as IBA500), was chosen for further characterization and adsorption tests. Due to a high content of maghemite, this sample showed weak magnetic properties (which were not the point of the study) and should be later used for its separation from the medium or fixation in filtration columns.

The ratio of P, S, and Cl to the iron content in samples annealed at 500°C for 180 min seem to be constant, thus the inorganic character of these elements is favored. In annealed samples, however, a rapid increase in calcium content was observed. As the sludge sampling was performed over the interval of several workdays, this is mostly affected by unpredicted changes in pH value of treated wastewater. Comparing the results for annealed and non-annealed samples (compare Tables 2 and 3), the total mass loss during annealing represents approximately 60%–65%, which corresponds to the sum of light elements; except for oxygen.

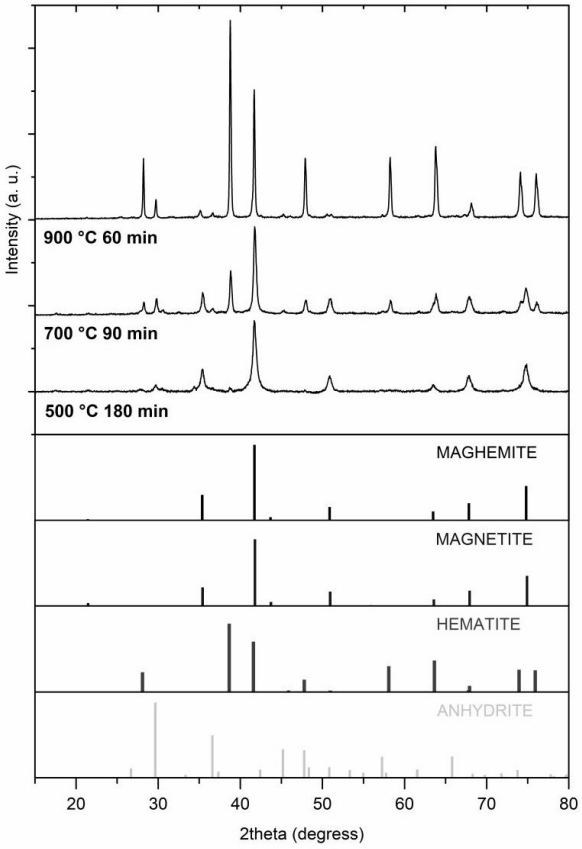

Fig. 3. XRD patterns of the dried sludge annealed at different temperature for various times.

Table 3
Amounts of selected elements determined by XRF measurement performed on the IBA500 sample

Sample	Element – ppm (ug/g)									
	P	S	Cl	K	Ca	Ti	Mn	Fe*	Sb	∑O
No. 1	7,358	18,693	3,139	2,759	38,952	3,570	878	553,000	1,441	xxx
No. 2	8,735	22,321	4,088	2,917	46,084	4,459	1,047	542,000	1,680	xxx
No 3	8,408	22,287	4,012	3,191	45,051	4,195	1,001	543,000	1,386	xxx
No. 4	8,213	22,344	4,365	3,149	44,175	4,214	998	498,000	1,370	xxx
Average	8,178	21,411	3,901	3,004	43,565	4,110	981	534,000	1,469	xxx
Percentage	0.81%	2.10%	0.39%	0.30%	4.36%	0.41%	0.10%	53.40%	0.15%	37.98%

*The amount of iron in the annealed samples was determined by EDX analysis due to the limitation of XRF spectrophotometer.

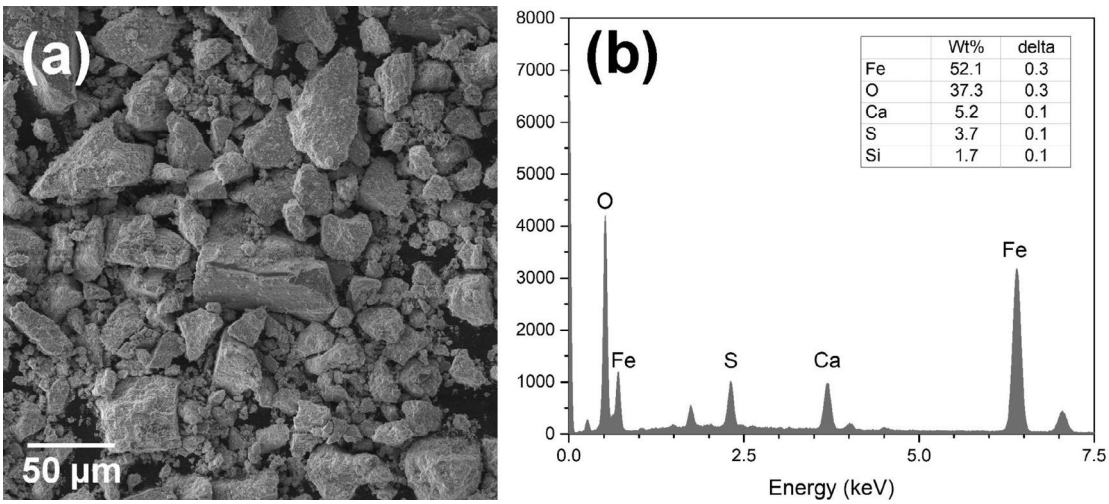

Fig. 4. Morphology and composition of the IBA500 sample studied by SEM (a) and EDX analysis (b).

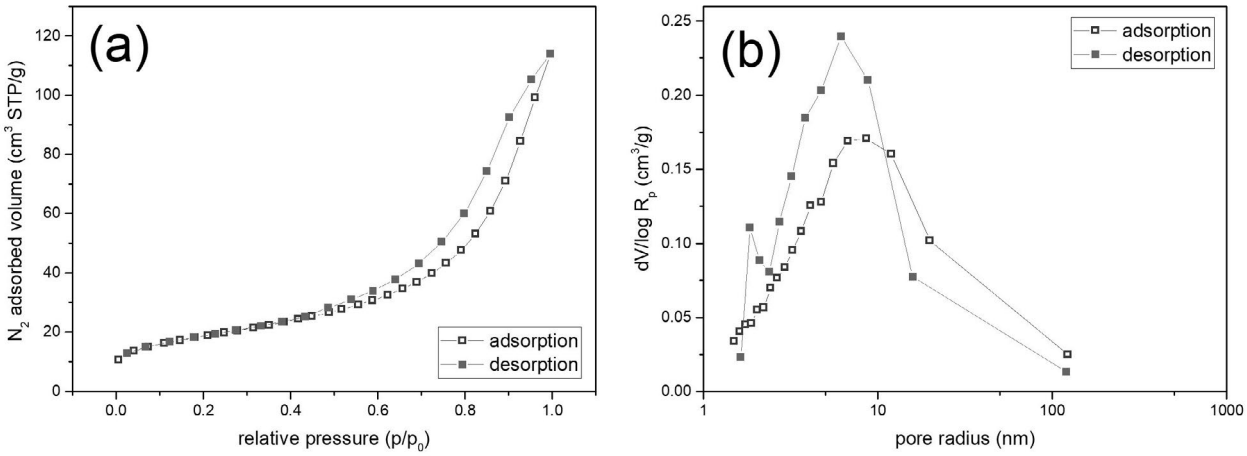

Fig. 5. Nitrogen adsorption isotherms of the IBA500 sample (a) and pore size distribution curves (b)

Table 4
Textural parameters of studied adsorbent

Sample	S_{BET} [m²/g]	V_a [cm³/g]	V_{micro} [cm³/g]	S_t [m²/g]
IBA500	66	0.1761	0.0026	59.6

Detailed morphology of the IBA500 sample observed by SEM is presented in Fig. 4a. The point, as well as mapping mode of the EDX analysis, confirmed the high amount of iron and oxygen, Fig. 4b, what pointed at the presence of predominant content of iron oxides/hydroxides, observed in the form of agglomerated particles creating bigger shapes with different dimensions. Feasibly, from further nitrogen adsorption analysis, it can be assumed that the iron oxides are approximately spherical particles of nanometer sizes.

The measured adsorption/desorption isotherm is presented in Fig. 5a. The adsorbed gas volume increased moderately, up to relative pressure $p/p_0 = 0.7$, then higher uptake was observed. The hysteresis loop between the adsorption and desorption branch is similar to the type *H*1, according to the IUPAC report [14], which is typical for materials with a tendency to create agglomerates. In general, the hysteresis loop is associated with the presence of mesopores (pores with the diameter in the range 2–50 nm) in the studied structure. Whereas the iron oxide particles are non-porous and have the tendency to create agglomerates, the presence of a hysteresis loop pointed to the mesopore structure forming between the particles, in the interparticle space. The textural parameters of the studied sample are given in Table 4. The value of the specific surface area of the sorbent material, S_{BET} = 66 m²/g, is only a bit lower than the values published for the synthetic nano-sized iron oxides (maghemite, magnetite), Table 5. This difference is due to the presence of other compounds in the industrial sample with a lower specific surface area. This fact corresponds, with the result of the XRD analysis and confirms the presence of the mentioned predominated iron oxide phases in the sample. The pore size distribution curve (Fig.

5b) showed a broader peak in the range of smaller up to larger mesopores, from 4.8 to 30 nm, with a maximum at 12.2 nm. Additionally, larger pores should be expected. A value of total pore volume V_a = 0.1761 cm^3/g was obtained for this material. Considering the shape of the diffraction lines of the reflections of the sample heated at 500°C and the pore size distribution of this sample, the nano-sized iron oxides particles should be present. The sorbent sample did not contain micropores (pores with width up to 2 nm). Its calculated value, V_{micro} = 0.0026 cm^3/g, was below the determination limit of the volume of micropores.

The physical characteristics of the adsorbent material and its chemical stability in various environments are crucial aspects for its possible large-scale application. While the iron oxides represent stable phases, which are slowly etched only in highly acidic conditions, the antimony present in the samples can be leached in both acidic and basic conditions. The leaching of metals into treated water during adsorption process is an unwanted phenomenon. The current allowable level of antimony in drinking water (according to the WHO) is set to 5 μg/L. To test stability, the adsorbent material was placed into different solutions of hydrochloric acid and sodium hydroxide for 8 h. It can be seen from the data given in Table 6 that antimony leached out from the adsorbent and its contents exceed limit values at the extreme points. On the other hand, high levels of iron represent a risk as well. In highly acidic conditions, the adsorbent materials deteriorate quickly, so the adsorbent cannot be used repeatedly.

Table 5
Comparison of the values of specific surface area for synthetized iron oxides

Material	S_{BET} [m^2/g]	Reference
Maghemite	81	[15]
Iron oxide 85	80	[16]
Iron oxide 20	76	[16]
Hydrophilic magnetite nanoparticles	72	[17]
Iron oxide pure	66	[18]
Freeze-dried maghemite	178	[19]
Magnetite nanoparticles	92	[20]
IBA500	66	In this study

Table 6
Leaching of iron and antimony into aqueous environment (different pH conditions) from IBA500 sample

Reagent	C_{Fe} (μg/L)	Fe	C_{Sb} (μg/L)	Sb
1 M HCl	21,300	30.32%	43.1	5.74%
0.1 M HCl	2,430	3.46%	<LOD	–
0.01 M HCl	935	0.90%	<LOD	–
Tap water	<LOD	–	<LOD	–
0.01 M NaOH	<LOD	–	16.8	2.24%
0.1 M NaOH	<LOD	–	21.4	2.85%
1 M NaOH	150	0.21%	23.5	3.13%

3.2. Adsorption tests

3.2.1. Zeta potential and effect of pH on adsorption properties

Fig. 6 shows the zeta potential of the studied adsorbent. The sample had a negative charge in the whole studied pH range and did not reach the point of zero charges. Generally, the synthetic iron oxides like magnetite or maghemite show one or two isoelectric points (IEP). The studied adsorbent material was prepared by thermal processing of the sludge obtained as a by-product of water treatment technology. Treated wastewater contained a significant amount of organic contaminants so that their residue in the material could affect the surface charge. The zeta potential was negative in the whole studied pH range and no IEP was observed. Since the entire charge of the composite is negative, maghemite/magnetite represents positively charged sites in the composite. These parts can interact with anionic species (e.g., arsenic oxyanions). According to the measured data, the adsorbent material should be slightly more effective in the suspensions of pH up to 7.

The pH of the solution influences the adsorption of toxic elements by adsorbents. The As(V) anions are present in aqueous solution in different forms depending on the pH of the solution. The pH value can also affect the degree of ionization of functional groups, the surface charge of the adsorbent, and the interaction between the ions and adsorbent. Compared to the model solution, the uptake of As(V) from the real wastewater showed different pH dependence. The adsorbent was shaken in the suspensions for 24 h to reach adsorption equilibrium. For the wastewater, the amount of adsorbed As(V) decreased with the increasing pH. For the model solutions, the adsorption effect was almost equal to pH 5 and 7 (Fig. 7). Comparing the real wastewater and the model solution, the value of adsorption capacity 700 and 860 μg/g was obtained at pH 7, respectively. Because the pH value of the real wastewater was about 7, further experiments (effect of adsorbent dosage and kinetic study) were performed without pH pre-treatment.

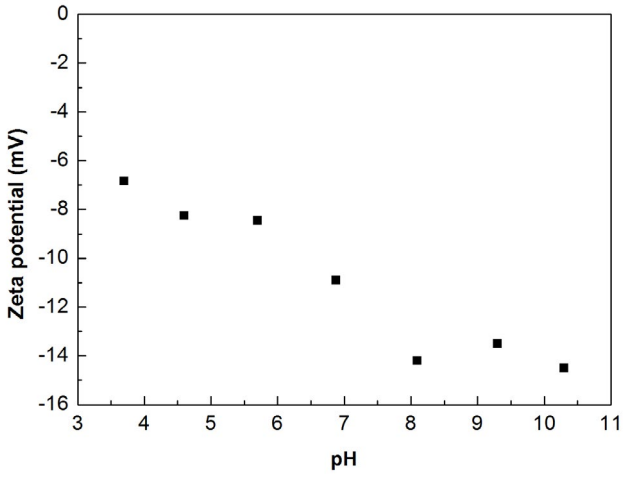

Fig. 6. Zeta potential of IBA500 sample at different pH values.

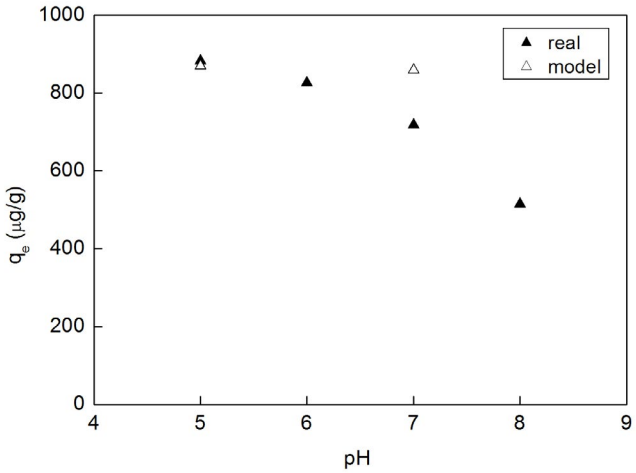

Fig. 7. Effect of pH on the adsorption of As(V) from the model solution and real waste water by IBA500 sample.

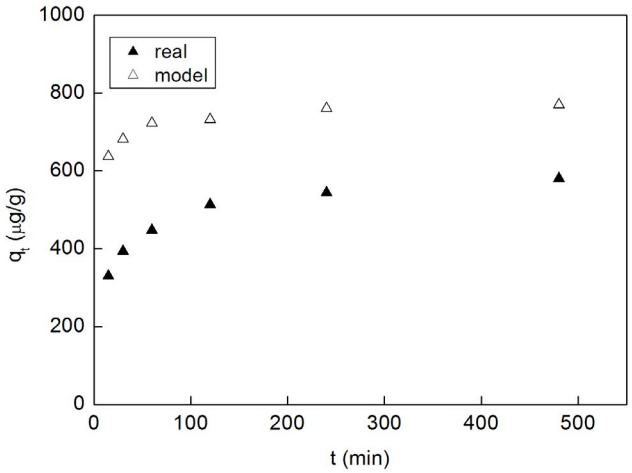

Fig. 9. Effect of contact time on the adsorption of As(V) from the model solution and real waste water by IBA500 sample.

Table 7
Kinetic parameters of pseudo-second-order model for the As(V) adsorption from the real waste water and model solution

	k (g/mg/min)	q_e (mg/g)	R^2
Waste water	0.097	0.596	0.9994
Model solution	0.273	0.776	0.9999

R^2 – coefficient of reliability.

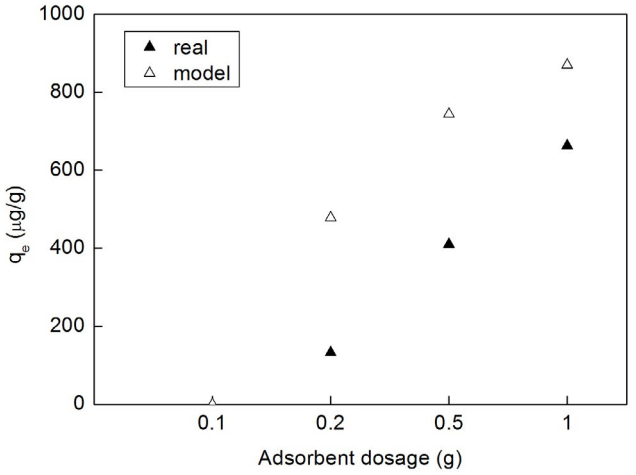

Fig. 8. Effect of adsorbent dosage on the adsorption of As(V) from the model solution and the real waste water by IBA500 sample.

3.2.2. *Effect of adsorbent dosage*

Fig. 8 shows the effect of various adsorbent loads on the As(V) removal from the real wastewater as well as from the model solution. The removal effect increased with increasing adsorbent dosage. The higher amount of As(V) was removed from the model solutions. Probably, the presence of other competitive ions (especially Cu, Ni, and Cd) in the wastewater may have influenced the As(V) adsorption. The differences between the adsorbed amounts were lower by increasing the adsorbent dosage.

3.2.3. *Adsorption kinetics*

The kinetics of As(V) adsorption were studied during 480 min. The uptake was analyzed in six different time intervals. Higher As(V) uptake was observed for the model solution compared to the wastewater. The equilibrium was reached at about 8 h of adsorption, Fig. 9. To analyze the kinetics of adsorption, the pseudo-second-order model was used to interpret the experimental data, Eq. (1):

$$\frac{t}{q_t} = \frac{1}{k q_e^2} + \frac{1}{q_e} t \tag{1}$$

where q_e and q_t are the amounts of metal ions adsorbed per unit mass (mg/g) at equilibrium and at any time t, respectively, k is the rate constant for the adsorption process (g/mg/min) [21].

The plots of the applied model to the experimental data are shown in Fig. 10. The kinetic parameters are given in Table 7. The results indicate that the sorption is governed by the pseudo-second-order reaction and the rate-limiting step may be chemical adsorption. The calculated value of the adsorbed amount at equilibrium was slightly higher for the adsorption from the model solution. The studied adsorbent removed approximately 50% of arsenate present in the wastewater. Based on the obtained results it can be concluded that iron-sludge material should be a convenient adsorbent for wastewater treatment.

4. Conclusion

The studied sorbent material was prepared from the iron-based sludge formed as a by-product of an industrial wastewater treatment technology. The material prepared at 500°C was a compact mixture of nanocrystalline

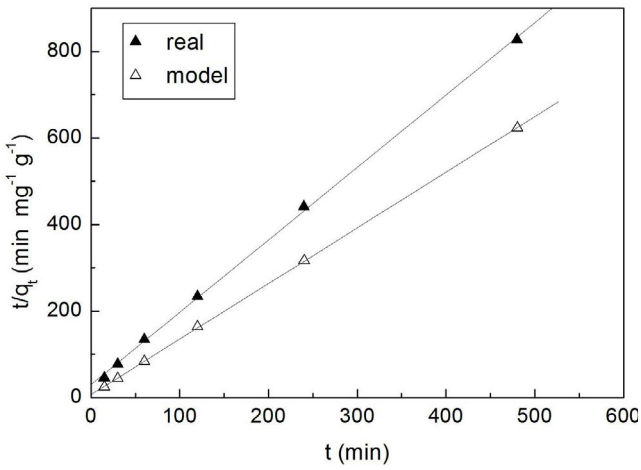

Fig. 10. Plots of the pseudo-second-order kinetic model applied on the adsorption data for As(V) removal from the model solution and real waste water by IBA500 sample.

anhydrite–maghemite–magnetite forming micrometric non-porous agglomerates. The adsorption tests proved the material to be efficient sorbent for As(V) removal. The real wastewater tests without any previous pre-treatment revealed maximum As(V) uptake to be 700 μg/g. It is believed that the measured value can be increased in the future by (a) pre-treatment of remediated water and (b) further modification of the iron-sludge waste recycling process. Due to its magnetic nature, it can easily be separated from the medium after the sorption process, or it can be kept in columns by a high gradient magnetic field without the bearer. In addition, the material was prepared from waste iron-based sludge which significantly reduced the overall costs for its production. Hypothetically, in this case, approximately 1 ton of adsorbent material could be produced per week from pressed sludge in a batch operational mode. Only moderate temperatures (400°C–500°C) are needed for the full conversion of raw sludge into the sorbent material such that the process remains economically feasible. The presented approach may inspire new ideas for recycling chemical wastes from remediation processes.

Acknowledgment

The authors are thankful for financial support of Grant Agency of the Slovak Republic VEGA for the projects No. 2/0029/19 and No. 2/0175/17. This work was realized within the frame of the project "Research Centre of Advanced Materials and Technologies for Recent and Future Applications" "PROMATECH," ITMS 26220220186, supported by the Operational Program "Research and Development" financed through European Regional Development Fund. A special thanks goes to Connie Massimino for language correction.

Symbols

S_{BET} — specific surface area, m^2/g
V_a — total pore volume, cm^3/g
V_{micro} — volume of micropores, cm^3/g
R^2 — coefficient of regression
t — time, hrs
q_e — amounts of metal ions adsorbed per unit mass at equilibrium, mg/g
q_t — amounts of metal ions adsorbed per unit mass at any time, mg/g
k — rate constant for the adsorption process, g/mg/min

References

[1] P. Xu, G.M. Zeng, D.L. Huang, C.L. Feng, S. Hu, M.H. Zhao, C. Lai, Z. Wei, C. Huang, G.X. Xie, Z.F. Liu, Use of iron oxide nanomaterials in wastewater treatment: a review, Sci. Total Environ., 424 (2012) 1–10.
[2] J. Hu, G. Chen, I.M.C. Lo, Selective removal of heavy metals from industrial wastewater using maghemite nanoparticle: performance and mechanisms, J. Environ. Eng., 132 (2006) 709–715.
[3] Z. Cheng, A.L.K. Tan, Y. Tao, D. Shan, K.E. Ting, X.J. Yin, Synthesis and characterization of iron oxide nanoparticles and applications in the removal of heavy metals from industrial wastewater, Int. J. Photoenergy, 2012 (2012) 5.
[4] M. Zhang, B. Gao, S. Varnoosfaderani, A. Hebard, Y. Yao, M. Inyang, Preparation and characterization of a novel magnetic biochar for arsenic removal, Bioresour. Technol., 130 (2013) 457–462.
[5] Z. Wu, W. Li, P.A. Webley, D. Zhao, General and controllable synthesis of novel mesoporous magnetic iron oxide@carbon encapsulates for efficient arsenic removal, Adv. Mater., 24 (2012) 485–491.
[6] C.-Y. Cao, J. Qu, W.S. Yan, J.F. Zhu, Z.Y. Wu, W.G. Song, Low-cost synthesis of flowerlike α-Fe_2O_3 nanostructures for heavy metal ion removal: adsorption property and mechanism, Langmuir, 28 (2012) 4573–4579.
[7] J. Hu, I.M.C. Lo, G. Chen, Comparative study of various magnetic nanoparticles for Cr(VI) removal, Sep. Purif. Technol., 56 (2007) 249–256.
[8] S. Martines-Vargas, A.I. Martínez, E.E. Hernández-Beteta, O.F. Mijangos-Ricardez, V. Vázquez-Hipólito, C. Patiño-Carachure, H. Hernandez-Flores, J. López-Luna, Arsenic adsorption on cobalt and manganese ferrite nanoparticles, J. Mater. Sci., 52 (2017) 6205–6215.
[9] S.R. Chowdhury, E.K. Yanful, Arsenic and chromium removal by mixed magnetite-maghemite nanoparticles and the effect of phosphate on removal, J. Environ. Manage., 91 (2010) 2238–2247.
[10] J. Liu, Z. Zhao, G. Jiang, Coating Fe_3O_4 magnetic nanoparticles with humic acid for high efficient removal of heavy metals in water, Environ. Sci. Technol., 42 (2008) 6949–6954.
[11] B. An, Q. Liang, D. Zhao, Removal of arsenic(V) from spent ion exchange brine using a new class of starch-bridged magnetite nanoparticles, Water Res., 45 (2011) 1961–1972.
[12] B.I. Kharisov, H.V. Rasika Dias, O.V. Kharissova, V.M. Jiménez-Pérez, B.O. Pérez, B.M. Flores, Iron-containing nanomaterials: synthesis, properties, and environmental applications, RSC Adv., 2 (2012) 9325–9358.
[13] S. Nizamuddin, M. Siddiqui, N. Mubarak, H. Baloch, E. Abdullah, S. Mazari, G. Griffin, S. Madapusi, A. Tanksale, Iron Oxide Nanomaterials for the Removal of Heavy Metals and Dyes from Wastewater, S. Thomas, D. Pasquini, S.-Y. Leu, D.A. Gopakumar, Eds., Nanoscale Materials in Water Purification, Elsevier Inc., Netherlands, 2019, pp. 447–472.
[14] K.S.W. Sing, Reporting physisorption data for gas/solid systems with special reference to the determination of surface area and porosity (Recommendations 1984), Pure Appl. Chem., 57 (1985) 603–619.
[15] A. Mockovčiaková, M. Matik, Z. Orolínová, P. Hudec, E. Kmecová, Structural characteristics of modified natural zeolite, J. Porous Mater., 15 (2008) 559–564.
[16] Z. Orolínová, A. Mockovčiaková, Structural study of bentonite/iron oxide composites, Mater. Chem. Phys., 114 (2009) 956–961.

[17] N.C.C. Lobato, M.B. Mansur, A.d.M. Ferreira, Characterization and chemical stability of hydrophilic and hydrophobic magnetic nanoparticles, Mater. Res., 20 (2017) 736–746.
[18] L.C.A. Oliveira, R.V.R.A. Rios, J.D. Fabris, K. Sapag, V.K. Garg, R.M. Lago, Clay-iron oxide magnetic composites for the adsorption of contaminants in water, Appl. Clay Sci., 22 (2003) 169–177.
[19] J. Hu, G. Chen, I.M.C. Lo, Removal and recovery of Cr(VI) from wastewater by maghemite nanoparticles, Water Res., 39 (2005) 4528–4536.
[20] B.E. Monárrez-Cordero, P. Amézaga-Madrid, C.C. Leyva-Porrasa, P. Pizá-Ruiza, M.M. Yoshida, Study of the adsorption of arsenic (III and V) by magnetite nanoparticles synthetized via AACVD, Mater Res., 19 (2016) 103–112.
[21] B. Erdem, A. Özcan, Ö. Gök, A.S. Özcan, Immobilization of 2,2′-dipyridyl onto bentonite and its adsorption behavior of copper(II) ions, J. Hazard. Mater., 163 (2009) 418–426.